International Journal of Greenhouse Gas Control 49 (2016) 413–424

International Journal of Greenhouse Gas Control

journal homepage: www.elsevier.com/locate/ijggc

Assessing induced seismicity risk at CO_2 storage projects: Recent progress and remaining challenges

Joshua A. White [a,*], William Foxall [b]

[a] Lawrence Livermore National Laboratory, Livermore, CA, USA
[b] Lawrence Berkeley National Laboratory, Berkeley, CA, USA

ARTICLE INFO

Article history:
Received 29 October 2015
Received in revised form 11 March 2016
Accepted 17 March 2016
Available online 13 April 2016

Keywords:
Carbon capture and storage
Induced seismicity
Risk assessment

ABSTRACT

It is well established that fluid injection has the potential to induce earthquakes—from microseismicity to magnitude 5+ events—by altering state-of-stress conditions in the subsurface. This paper reviews recent lessons learned regarding induced seismicity at carbon storage sites. While similar to other subsurface injection practices, CO_2 injection has distinctive features that should be included in a discussion of its seismic hazard. Induced events have been observed at CO_2 injection projects, though to date it has not been a major operational issue. Nevertheless, the hazard exists and experience with this issue will likely grow as new storage operations come online. This review paper focuses on specific technical difficulties that can limit the effectiveness of current risk assessment and risk management approaches, and highlights recent research aimed at overcoming them. These challenges form the heart of the induced seismicity problem, and novel solutions to them will advance our ability to responsibly deploy large-scale CO_2 storage.

1. Introduction

Geologic carbon storage is a valuable strategy to reduce atmospheric CO_2 emissions while minimizing the economic disruption of de-carbonizing the world's energy supply (International Energy Agency, 2010; Pacala and Socolow, 2004). Like all technologies, however, sequestration projects create a number of environmental and safety hazards that must be addressed. These include the potential for injection-induced earthquakes, which result from altering pore-pressure and state-of-stress conditions in the subsurface. To date, measured seismicity due to CO_2 injection has been limited to microseismicity and a few felt events (see Table 1). The hazard exists, however, and must be addressed. There are important similarities between CO_2 injection and fluid injection for other energy technologies that have induced significant events—e.g. geothermal systems, waste-fluid injection, hydrocarbon extraction, and others (National Research Council, 2012). There are also important distinctions among these technologies that should be considered in a discussion of inherent seismic risk (IEAGHG, 2013).

This paper discusses strategies for assessing induced seismicity risk during each phase of a geologic carbon storage (GCS) or CO_2-enhanced oil recover (CO_2-EOR) project. Before beginning, we note that *risk assessment* is only the first part of a broader *risk management* strategy. That is, the likelihood of inducing earthquakes and the ensuing risk at a given project are not fixed quantities, and can be lowered using a mix of mitigation and remediation strategies. To keep the discussion focused, however, we limit ourselves here to the assessment piece. A careful assessment of evolving risk at a site should inform all decision-making, and is therefore an essential first step towards effective management (Pawar et al., 2015; White and Foxall, 2014).

We employ the general notion that *risk* consists of three parts (Kaplan and Garrick, 1981):

1. one or more scenarios of concern;
2. the probability of a given scenario occurring;
3. and the damage that would result (i.e. the consequence of the scenario).

Thus a quantitative measure of risk must encompass both the probability of an event and the severity of its impacts. The term *hazard* is used to refer to components 1 and 2 alone—i.e. just the probability of occurrence, without the measure of damage.

The first step in a risk assessment is identifying all plausible scenarios that may lead to damage. For a CO_2-injection project, four

* Corresponding author.
E-mail address: jawhite@llnl.gov (J.A. White).

http://dx.doi.org/10.1016/j.ijggc.2016.03.021

Table 1
Summary of seismicity observations at recent CO_2 injection operations.

Project	Category	Monitoring design	Observations [a]	Seismicity Type[b]	References
Aneth USA	CO_2-EOR	Borehole Array	Magnitudes: **M**-1.2 to **M**0.8 Frequency: 3800 events over 1 year. Two fault-like clusters.	II	Rutledge (2010), Zhou et al. (2010), Soma and Rutledge (2013)
Cogdell USA	CO_2-EOR	Regional Network	One **M**4.4 event and 18 magnitude 3+ events over a 6 year period. No major seismicity at nearby, similar operations.	I	Gan and Frohlich (2013), Davis and Pennington (1989)
Weyburn Canada	CO_2-EOR	Borehole Array	Magnitudes: **M**-3 to **M**-1. Frequency: 100 events over 7 years. Diffuse locations.	II	Whittaker et al. (2011), White et al. (2011), Verdon et al. (2010, 2011)
Decatur USA	Dedicated Storage	Borehole Arrays Surface Stations	Magnitudes: **M**-2 to **M**1 Frequency: 10,123 events over 1.8 years. Multiple fault-like clusters.	I	Will et al. (2014), Couëslan et al. (2014), Kaven et al. (2014, 2015)
In Salah Algeria	Dedicated Storage	Borehole Array	Magnitudes: **M**-1 to **M**1. Frequency: 5500 events over 2 years. Indications of fracture stimulation.	I & II	Oye et al. (2013), Goertz-Allmann et al. (2014), White et al. (2014b), Verdon et al. (2015)

[a] **M** = moment magnitude.
[b] Type I = seismicity concentrated within overpressured zone. Type II = seismicity outside overpressured zone.

scenarios related to fault reactivation and induced seismicity are of primary concern. Induced slip on faults could potentially lead to:

1. property damage;
2. a public nuisance;
3. brine-contaminated drinking water;
4. and CO_2-contaminated drinking water.

The four scenarios lead to different types of damage: to property, to drinking water quality, or to the public well being. The first scenario (property damage) is analogous to the risk associated with natural seismicity, though here building and infrastructure damage results from induced events. The second scenario captures the notion that felt earthquakes will bother people in the local vicinity, even if there is no permanent damage. In this paper we use the common terminology "nuisance" for this risk, though unfortunately this word may convey the sense that it is a minor problem. The consequences should not be underestimated, however, as public backlash can lead to projects being shut down (Deichmann and Giardini, 2009) or skepticism of geologic carbon storage as a safe technology (Singleton et al., 2009). Scenarios 3 and 4 result from the observation that slip in a fault zone can alter its permeability structure, potentially creating or reactivating leakage pathways (Zoback and Gorelick, 2012, 2015; Juanes et al., 2012; Vilarrasa and Carrera, 2015a,b). It is helpful, however, to make a distinction between brine and CO_2 leakage. While they may occur together, they have different physical behavior, likelihoods of occurrence, and groundwater impacts. In the case that other in situ fluids are present—e.g. oil or gas—additional scenarios could be added. Indeed, the enumeration of risks above is not meant to be exhaustive, and additional risk scenarios may be important at a given site. The four listed here, though, are key priorities for all onshore storage operations. Also, while the intrinsic damage potential of offshore CO_2 storage may be much lower, significant fault reactivation and induced seismicity in an offshore project is also undesirable.

Given these four scenarios, this paper focuses on strategies for assessing their likelihoods of occurrence and the damage that may result. Ultimately, mitigation techniques can be applied to both aspects—i.e. safeguards can be put in place either to lower the likelihood of significant seismicity or to minimize damage should earthquakes occur. While it is desirable to avoid induced seismicity in the first place, the inherent complexity of subsurface systems make this a challenging task. Selection of sites having certain formation characteristics and operational procedures can be used to lower this likelihood, but an irreducible chance of inducing larger earthquakes will always remain. In light of this, it is pragmatic to always choose sites and engineering safeguards such that consequences will be low even if unwanted events occur.

The paper begins with a brief overview of the fundamental mechanisms behind induced seismicity, with a focus on the mechanics of CO_2 storage. We then review observations of induced earthquakes to date at recent CO_2 injection and comparable operations. This science basis—and its gaps—is crucial because it points to critical challenges in effectively implementing risk assessment approaches. The paper then presents a high-level overview of the key elements that inform a seismic risk assessment. We adopt one particular framework, Probabilistic Seismic Risk Assessment, but the underlying hazard and risk elements are universal and will be present in alternative assessment approaches.

The heart of the paper then describes key challenges in actually implementing such an assessment framework. In essence, geophysical characterization and monitoring limitations introduce very large uncertainties in the inputs to the risk assessment, and novel strategies are necessary for reducing and/or circumventing these uncertainties. We describe recent research by various groups that have made progress tackling these challenges, and also highlight open questions that remain. We conclude the paper with a list of research fronts that the authors feel will significantly advance our ability to assess and manage seismicity risk at CO_2 storage operations moving forward. The ultimate goal is to ensure we can deploy this valuable technology in a safe and responsible manner.

2. Mechanics of induced seismicity

Fig. 1 provides a conceptual illustration of the basic seismicity concern at a CO_2 storage site. Here, a well injects supercritical CO_2

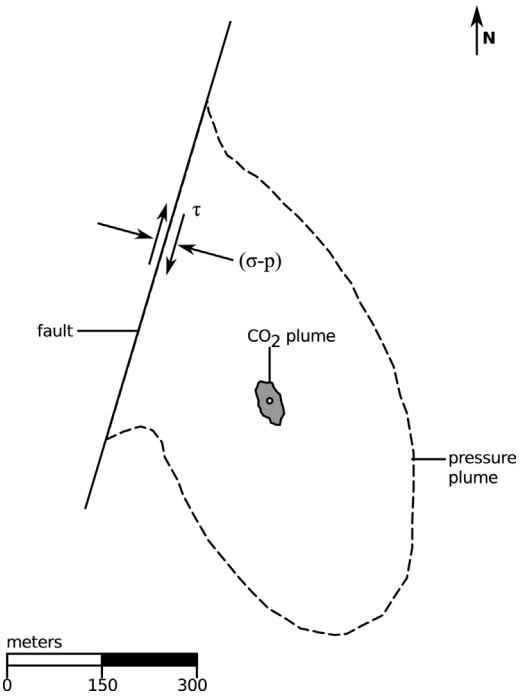

Fig. 1. Plan view of a CO_2 storage reservoir, showing pressure interaction between a vertical well and nearby fault.

into a storage reservoir. The reservoir is intersected by a moderately large, pre-existing fault. As injection begins, a CO_2-rich plume grows away from the injector, driven by pressure gradients and buoyancy forces. As the injected fluid displaces the in situ brine, a large overpressure plume also develops. Note that the extent of the pressure perturbation is typically much larger than the CO_2-rich plume. This pressure perturbation plume can interact with the fault, and potentially trigger seismic or aseismic slip.

A simple Coulomb criterion is often used to express the condition for fault stability (Scholz, 2002),

$$\tau \leq \mu(\sigma - p) \tag{1}$$

Here, τ and σ are the total shear and normal tractions applied on the fault, p is the pore fluid pressure, and μ is the static friction coefficient. The geomechanical convention is that positive stresses are compressive. The quantity $\sigma' = (\sigma - p)$ represents the *effective* normal traction on the fault, which is reduced by an increase in pore pressure or by a reduction in the in situ confining stress. The stability condition states that the fault will be stable as long as the shear traction is less than the current shear strength—i.e. the right hand side of Eq. (1). Here, we neglect any additional contribution to shear strength from fault cohesion, though this effect can be included as necessary.

We note that the deformation of the reservoir and density-change effects can create poromechanical stress perturbations that extend beyond the overpressured zone. These far-field stress perturbations can potentially reactivate well-oriented faults and fractures without substantially altering the local pore pressure p at the fault. For example, there are well known cases of production-induced seismicity, when net volume change in the reservoir is negative (Segall, 1989). As a convenient shorthand, we will refer to seismicity induced by direct pressure communication with faults as Type I seismicity, and seismicity induced outside of the overpressured zone as Type II.

The shear and normal tractions resolved on a fault plane will depend on the in situ state of stress in the formation, stress perturbations due to injection and/or production, and on the orientation

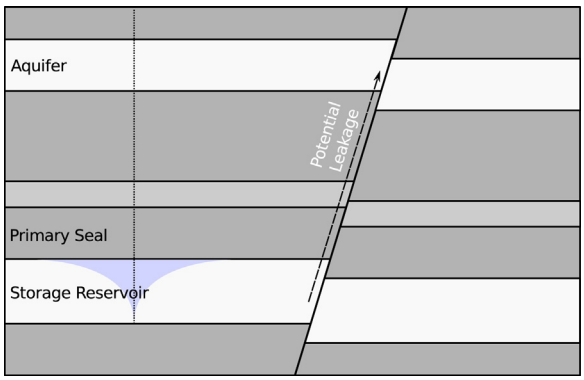

Fig. 2. Section view of a large fault intersecting a storage reservoir and shallow aquifer (not to scale). With this geometry, fault rupture could enhance the potential for leakage out of the storage zone.

of the fault with respect to this stress state. For a given state of stress, some faults may be favorably oriented for slip, while others may be poorly oriented. A simple measure of fault stability is therefore the critical pore pressure change Δp (or effective stress perturbation $\Delta\sigma'$) required to make condition (1) an equality. It is commonly observed that many faults are naturally in a state of critical equilibrium, in which the equality condition is nearly satisfied under in situ stresses and formation fluid pressures (Zoback and Townend, 2001). Very small perturbations in stress or pore pressure therefore can induce slip. It is these critically stressed faults that pose the greatest challenge for subsurface fluid injection (Zoback and Gorelick, 2012).

Eq. (1) is a useful simplification, though it masks some of the underlying complexity of fault reactivation. For example, this criterion is expressed as a point-wise condition, whereas in reality the stability of the fault will depend on a distribution of stresses, pressures, and friction strength across the whole structure. A variety of poromechanical and thermomechanical effects may substantially alter the state of stress in the reservoir and surrounding formations. Also, this condition only describes the behavior of the fault while it is in static equilibrium. Once slip is initiated, the fault may creep aseismically until it reaches a new stable configuration (quasi-static slip) or rupture dynamically in an earthquake (Dieterich, 1979; Ruina, 1983; Scholz, 2002). Strain accumulation during individual ruptures will also modify the state of the fault and nearby neighbor faults, potentially leading to complex foreshock/mainshock/aftershock cascades—e.g. (Sumy et al., 2014; Dieterich et al., 2015).

A related concern is that reactivation of a fault can create new permeable pathways, though the fault must penetrate the entire caprock seal (or seals) in order to create a leakage concern (Fig. 2). Given that the total area of the pressure perturbation plume is typically much larger than the mobile CO_2 plume, at many sites the risk of brine leakage may actually be much larger than CO_2 leakage risk, as mobile CO_2 may never come in contact with the reactivated fault. Both CO_2 and brine can cause groundwater degradation, and both types of leakage are a key project design factor. It is useful to distinguish them, however, as leak detection and management strategies for the two leakage types differ somewhat. Brine leakage requires a pressure differential to sustain it, while CO_2 leakage can rely on buoyancy drive alone. Also, the time periods of concern differ. Brine leakage can be effectively halted by reducing the driving pressure gradient. Removing pressure drive will also slow CO_2 leakage, but buoyancy drive may allow it to persist indefinitely until other trapping or remediation mechanisms come into play (Imbus et al., 2013; Zahasky and Benson, 2014).

Though the processes of fault reactivation, seismicity, and permeability change are closely related to each other, the occurrence

of one does not necessarily imply the occurrence of the others. For example, there could be fault reactivation with aseismic slip, fault reactivation with no substantial permeability change, and intrinsically permeable faults that have not experienced any reactivation. Faults that do not penetrate caprock seals may pose a seismicity hazard but will not create the same leakage hazard as a penetrating pathway. The depth, orientation, and lithologic composition of the fault is therefore crucial. In the event of rupture, the distribution of slip along the fault and any deformation in adjacent damage zones will control permeability modifications.

There are a number of CO_2-specific mechanisms that could potentially play a role in the seismic behavior of carbon storage operations, though direct observation of these mechanisms at field scale is challenging. For example, CO_2 can react chemically with certain fault minerals and potentially alter friction and permeability properties. Similarly, some clays may swell substantially in contact with supercritical CO_2, creating an additional stress perturbation. Given the relatively small size of the CO_2 plume in comparison to the pressurized brine volume, however, these additional effects—if they exist—would be confined to faults in closer proximity to the injection well.

3. Field experience

Field experience with CO_2 injection has grown in recent years, with new demonstration and commercial scale projects coming online. Specific studies on the seismic behavior at these fields, however, are more limited. Relatively few sites have deployed sensitive microseismic arrays capable of detecting smaller events. Table 1 summarizes seismicity observations at five CO_2 injection operations. The projects fall into two categories: CO_2-enhanced oil recovery projects (CO_2-EOR) and dedicated saline storage projects. Observed seismicity is denoted as Type I or Type II according to the broad classifications defined in Section 2.

The five projects summarized in Table 1 have shown a diverse range of seismic responses. We note that each site is unique and complex, and the brief notes given in Table 1 contain uncertainties and important caveats. The reader should consult the cited references for further details. Here, we briefly focus on three of these projects—Weyburn, Decatur, and Cogdell—as representative examples to highlight some unifying trends that have emerged in recent years.

The earliest CO_2-EOR project to deploy microseismic monitoring was the Weyburn–Midale CO_2 Monitoring and Storage Project in Saskatchewan, Canada (White et al., 2011). The Weyburn and Midale oil fields have a long history of EOR operations, with water flooding beginning in the 1960s. Starting in 2000, CO_2 has been injected to improve oil production. As of 2011, the total CO_2 injection rate reached 5.3 Mt/year through more than 100 wells (Whittaker et al., 2011). The net storage rate—i.e. excluding recycled CO_2—was 2.7 Mt/year. Injection rates for individual wells range from 50 to 500 tonnes/day. In August 2003, a deep borehole seismic monitoring array was deployed in an abandoned production well to study the behavior of one injection/production well pattern (Verdon et al., 2010, 2011). Between 2003 and 2010, approximately 100 locatable microseismic events were detected, with estimated moment magnitudes ranging from **M**-3 to **M**-1. The overall seismicity rate is therefore extremely low. While location uncertainties are large, most of these extremely small events appear to be diffusely located in the overburden and underburden, rather than localized to the reservoir interval. Geomechanical modeling suggests that the microseismicity is driven by stress perturbations due to reservoir deformation, rather than by direct pressure communication with the wells (Verdon et al., 2011). Many of these events are located in proximity to underpressured production wells, further supporting the Type II hypothesis. Similar indications of Type II seismicity have been associated with CO_2-EOR at the Aneth Oil Field in Utah (Rutledge, 2010; Zhou et al., 2010; Soma and Rutledge, 2013).

The Illinois Basin Decatur Project was the first large-scale dedicated storage demonstration in the U.S., injecting 1 Mt between 2011 and 2014 (Couëslan et al., 2014). CO_2 is stored in a 550 m thick, high-permeability sandstone unit at 2100 m depth. This saline aquifer (the Mt. Simon) is regionally extensive and has significant capacity for future storage operations. The pressurized storage zone directly overlies Precambrian granitic basement. Two independent groups have carried out microseismic monitoring at the site. The Decatur Project operates two deep borehole microseismic strings, one in the injection well and one in an offset monitoring well (Will et al., 2014; Couëslan et al., 2014). Separately, the U.S. Geological Survey (USGS) has installed a 12-station surface and shallow borehole array (Kaven et al., 2014, 2015). The deep borehole array has superior sensitivity to small events, while the surface array provides better spatial and focal sphere coverage. Both groups have observed clusters of microseismic events, several with linear trends and consistent Northeast strikes, near the bottom of the Mt. Simon and into the Precambrian basement. It appears that pressure from the storage operation has reactivated a number of small, well-oriented faults in the basement. No events have been seen in proximity to the upper seal, the Eau Claire Shale. The more sensitive downhole array has detected 10,123 events during 22 months of injection, with estimated magnitudes ranging from **M**-2 to **M**1. Location estimates for 2573 of these events reveal distinct microseismic clusters, with an expanding radius of seismic activity as injection proceeds. Several wastewater injection sites have observed similar microseismic clustering, notably the U.S. Bureau of Reclamation Paradox Valley Unit in Colorado (Ake et al., 2005; Block et al., 2012). Microseismic clusters that appear to define faults have also been observed at the Aneth Oil field, though these appear to have been activated in a Type II mode (Rutledge, 2010; Zhou et al., 2010; Soma and Rutledge, 2013).

The only case reported to date where earthquakes larger than **M**1 have been attributed to gas injection is at the Cogdell oilfield in Texas (Gan and Frohlich, 2013). A total of 38 earthquakes were recorded by the permanent regional seismic network and located within or close to the field during a period of high-rate gas injection between 2006 and 2011. Augmentation of the regional network coverage by stations of the Earthscope U.S. Temporary Array between 2009 and 2011 enabled a total of 105 events larger than about magnitude 1 to be located relatively accurately during this two-year period. Eighteen of the events detected by the permanent network had magnitudes between 3 and 4.4. If events within this range had occurred during the previous 20 years, most would have been detected by the network. Although previous earthquakes as large as magnitude 4.6 occurred in the vicinity of the Cogdell field during a period of waterflooding between 1956 and 1982 (Davis and Pennington, 1989), no seismicity was recorded in the area between 1983 and 2005.

Oil is produced at Cogdell from the Horseshoe Atoll limestone reef. Sustained CO_2 (and/or possibly methane) injection for EOR at a depth of about 2100 m began in 2001. The injection rate was increased sharply in 2003 to average about 350,000 m^3/month at the depth of injection until 2008. Five events ranging from magnitude 2 to 3.9 were recorded during this period, but almost all of the seismicity—including all but two of the magnitude 3+ events—was recorded during 2009 and 2010, when the injection rate peaked to average about 400,000 m^3/month. Seismicity continued to accompany injection at somewhat lower rates through 2011. Whereas water injection since 1976 has been approximately balanced by production, gas injection since 2001 has resulted in a net increase in reservoir fluid volume.

Most of the events located using US Array data occurred as five or six clusters, all of which are within four km of groups of injection wells. Three of the clusters define linear seismicity features having orientations that correspond to focal mechanism solutions for five larger events, which suggests that the seismicity occurred as triggered slip on previously unidentified faults. However, the network station spacing is too large to determine accurate earthquake focal depths, and hence the depths of the faults. It is pertinent to compare the apparent seismic response from gas injection at Cogdell with the lack of response at the Kelly-Synder field immediately to the southwest. Even though the Kelly-Synder field lies along the same structural trend as Cogdell and production is from the same limestone reservoir, no seismicity has been detected there despite closely similar trends in production and both water and gas injection histories at the two fields. The Kelly-Synder field was the site of the SACROC CO_2-EOR research project carried out by the DOE-sponsored Southwest Regional Partnership on Carbon Sequestration (Han et al., 2010). A detailed understanding of the key attributes leading to different seismic responses in these two fields is not yet available.

While the handful of case studies described above have improved our understanding of site-specific hazards, the overall empirical database of seismic events triggered by CO_2 injection is small. With limited data, it is difficult to make any overarching conclusions about the intrinsic seismic hazard associated with CO_2 storage. Further, even the examples described here display widely different responses. This is because hydromechanical behavior is highly site and operation-specific, as illustrated by the contrast between the Cogdell and Kelly-Synder fields. In this data-poor context, it would be valuable for future storage projects to deploy at least some baseline microseismic monitoring capability. This additional data can help identify and manage seismicity issues before they become a major operational problem.

4. Comparison with other injection technologies

The seismicity hazard associated with CO_2 injection is similar in many ways to that posed by subsurface injection for other purposes such as wastewater disposal, geothermal energy production, and reservoir stimulation by hydraulic fracturing or hydraulic shearing. Given limited experience so far with CO_2-induced events, it is important to learn as much as possible from these other practices. Clearly, however, there are features specific to each of these injection applications that will lead to differences in seismic hazard and risk; these include, for example, the hydromechanical properties of typical reservoir lithologies, injection rates and pressures, and net total volumes of injected fluid. Additional factors such as the degree of site characterization, the extent of site monitoring and permitting requirements also influence the way that seismic hazard assessments are carried out.

In its comprehensive review of induced seismicity related to energy technologies, the National Research Council (National Research Council, 2012) identified net fluid balance as the most important factor influencing the likelihood of induced seismicity—i.e. the net volume change resulting from both fluid injection and production. A more recent study (Weingarten et al., 2015) found that seismicity associated with wastewater disposal wells across the central U.S. is strongly correlated with the *rate* of fluid injection, rather than the accumulated net volume over decades-long time periods. Relatively sharp increases in net injection over time intervals shorter than the characteristic diffusion time scale will result in overpressure build-up, the primary driver of induced seismicity. Injection applications that result in low net fluid injected volumes, such as short-duration well stimulation and waterflood for EOR, typically create smaller and/or less intense overpressured zones, reducing the likelihood of Type I seismicity. The impact on Type II seismicity is less clear, however, because, as discussed in Section 2, any stress perturbation caused by injection and/or production can potentially reactivate well-oriented faults.

Consideration of net injected volume alone would imply that CO_2-EOR projects should have smaller seismic risk than dedicated storage. As Table 1 indicates, however, the largest earthquakes associated with CO_2 injection observed to date have occurred at the Cogdell CO_2-EOR field, suggesting that in this case the high injection rate (averaging about 400,000 m^3/month) during the seismicity sequence was the determining factor. This illustrates that multiple factors must be considered in a rigorous assessment of project risk. It is essential to investigate the likely spatial distribution, magnitude, and timing of stress perturbations that will be caused by injection and/or production operations. The stress perturbation field provides a more direct measure of reactivation potential. This detailed stress assessment is particularly important for fields that experience complex injection and production histories involving multiple wells and multiple fluids, such as CO_2-EOR operations.

Dedicated storage projects have raised concern because sequestering megatonnes (and ultimately, gigatonnes) of CO_2 in the subsurface will create large overpressured regions, increasing the likelihood that the overpressure will encounter larger faults capable of generating significant seismicity (Zoback and Gorelick, 2012, 2015; Juanes et al., 2012; Vilarrasa and Carrera, 2015a,b). The closest technology analog is waste-water disposal, which also involves injecting large volumes of fluid over significant time periods. In the U.S., a dramatic increase in the rate of seismicity has been observed in parts of the central and eastern U.S. since 2001, which is attributed to increased wastewater disposal activity resulting from the boom in unconventional shale oil and gas recovery enabled by hydrofracturing. The largest events to date that have been attributed to wastewater injection are **M**5.3 and **M**5.7 earthquakes that occurred in 2011 in Colorado and Oklahoma, respectively (Rubinstein et al., 2014; Keranen et al., 2013; Sumy et al., 2014).

According to Weingarten et al. (2015), induced events have been associated with only about 10% of the more than 180,000 Environmental Protection Agency (EPA) active or formerly active Class II (wastewater disposal and EOR) injection wells in the U.S. From a public engagement point of view, however, a handful of problematic projects has quickly gripped public attention. Given heightened scrutiny of CO_2 disposal as an unfamiliar technology, even one or two problematic projects may quickly create a public perception issue, even if the vast majority of storage operations experience no seismicity of concern whatsoever.

Weingarten et al. (2015) also point out that induced earthquakes are conspicuously absent in several regions in the central and eastern U.S., such as the San Juan Basin of New Mexico, the Williston Basin of North Dakota and large areas of the Gulf Coast, where thousands of wastewater and EOR wells are active. In California, Goebel et al. (2015, 2016) identified four earthquake sequences between 1975 and 2014 that were possibly associated with wastewater injection at oilfields in the southern San Joaquin Valley, but Goebel (2015) found no apparent large-scale correlation of seismicity with a marked overall increase in injected volumes since 2001. This is in contrast to Oklahoma, where average basin-wide injected volumes are roughly similar to those in California. While a great deal of further study is needed, these regional differences in seismic response might be due, at least in part, to fundamental differences in uppermost crustal stress states, geologic structure and hydraulic connectivity in different tectonic settings. Whatever the cause, it is fair to assume that there will be important regional differences in the hazard posed by induced seismicity.

Most industrial-scale dedicated storage projects currently under construction or in the planning stage have projected injection rates

between 1.0 and 3.5 Mt/year (or 1.4 and 5M m^3/year, assuming a density of 700 kg/m^3 for supercritical CO_2), injected through one or more wells. These rates are somewhat higher than typical high-volume wastewater injection rates—in the range of about 200,000–500,000 m^3/year—in areas of the central U.S. that have recently experienced induced seismicity. A few individual disposal wells in some of these areas inject at rates of 1–3M m^3/year. Furthermore, in some cases multiple nearby wells inject into the same target formation. For example, the cumulative injection rate in two adjacent injection wells within 2 km of an **M**4.7 foreshock of the 2011 **M**5.3 earthquake in Colorado was 63,100–76,100 m^3/mo (757,000–910,000 m^3/year) (Rubinstein et al., 2014), approaching the projected rates of planned CO_2 projects. Since wastewater disposal into some wells is continuous over time periods as long as decades, total reservoir volume changes can be of the same order (10–100M m^3) as the projected volumes of stored CO_2 of most of the planned GCS projects.

Most wastewater injection is into sedimentary formations in which pressure increases are moderated by relatively high permeabilities—similar to CO_2 storage. Although minor seismicity occurs within these units, in the documented cases to date the largest events (**M**3+) have occurred in the basement and/or lowermost sediments well below the injection interval. Pressure migration to deeper units with greater seismic potential is a key concern for CO_2 storage operations as well (Will et al., 2014).

One final factor controlling a project's seismic risk is the level of effort devoted to site selection, characterization, monitoring, and risk planning. Permit requirements under which the injection is carried out will therefore play an important role. In the U.S., for example, wastewater disposal and EOR operations require a Class II Underground Injection Control permit, while dedicated storage operations require a different Class VI permit (U.S. Environmental Protection Agency, 2012). The Class VI requirements are generally viewed as much more stringent. Given that only a few Class VI permits have been issued to date, however, the long term impact of different permitting and oversight requirements is as yet unclear.

5. Probabilistic Seismic Risk Assessment

Given the problem potentially posed by induced seismicity, an effective risk assessment and risk management framework is essential to project design. The two components—assessment and management—should go hand-in-hand in a closed-loop feedback cycle. This section gives an overview of the key elements that contribute to a project risk assessment. We describe a high-level workflow, setting the stage for a detailed discussion of challenges to implementing this workflow in Section 6. Risk assessment is a widely-studied field, with a significant body of practice to draw on to address the current problem. The true difficulty is ensuring the inputs to the chosen assessment workflow are meaningful. For induced seismicity applications, determining input parameters with acceptably narrow uncertainty bounds poses numerous hurdles.

A useful approach to assessing induced seismicity risk is to adapt the standard Probabilistic Seismic Risk Assessment (PSRA) approach widely used to estimate the risk of structural damage from naturally-occurring earthquakes. As certain regions are now dealing with both natural and induced events, a unified assessment framework is also desirable. PSRA involves coupling the probability of an event occurring with its societal consequences, which in the case of induced seismicity include nuisance caused by felt ground motion as well as building and infrastructure damage. PSRA is generally carried out using the following procedure:

1. *Source characterization*: Identify seismic sources, which may be individual faults or zones within which earthquake occurrence is assumed to be homogeneous.
2. *Earthquake occurrence rate*: Estimate the average frequencies of occurrence of earthquakes of different magnitudes for each source. These occurrence rates may contain time-dependencies and correlations between sources.
3. *Ground motion*: Calculate the ground shaking resulting from earthquakes on each source at sites of interest. Ground shaking measures include ground velocity and acceleration at specified frequencies, or seismic intensity. These are primarily functions of earthquake magnitude, source-to-site distance, and local site conditions.
4. *Hazard*: Derive a hazard curve representing the forecasted probability of exceeding each ground motion value, usually on an annual basis. This curve is derived by integrating the frequencies of occurrence of ground motions generated by all sources. In conventional PSRA, hazard constitutes a long-term forecast, typically over time periods of several decades. For induced seismicity, the hazard has an inherent time-dependency, and forecast windows must be adjusted accordingly.
5. *Vulnerability*: Develop a vulnerability function for each receptor (i.e. buildings, infrastructure, population centers) that expresses the probability of creating a certain level of damage or nuisance for a given ground motion value. Usually this involves structural analysis for buildings, or surveys asking people how they respond to given levels of shaking. Vulnerability functions are typically determined for different receptor "classes" (e.g. multi-story wood-framed homes). Custom vulnerability assessments are reserved for specialized assets.
6. *Risk*: Derive a risk curve representing the annual probability of a given consequence, such as a specified degree of structural damage. This is accomplished by convolving the hazard curve with the vulnerability function.

Steps 1–4 constitute a Probabilistic Seismic Hazard Assessment (PSHA), while Steps 5 and 6 add the damage component necessary for risk evaluation (PSRA). While we have adopted PSRA terminology here, these six elements are fundamental and will appear in one form or another in alternative assessment frameworks—whether they be quantitative, semi-quantitative, or qualitative.

Standard PSHA and PSRA methods require a number of modifications before they can be applied to induced seismicity. We will discuss these issues in more detail in Section 6, but two major changes are apparent:

First, source characterization and frequency-magnitude estimation (Steps 1 and 2) pose more of a challenge. For natural seismicity, there is often a long historical catalog of events we can use to identify sources and estimate long-term recurrence rates. Also, it is usually (though not always) assumed that these long-term rates are stationary in time. The hydromechanical processes responsible for induced seismicity, on the other hand, introduce strong time- and space-dependencies, and while in some instances background seismicity may aid in identifying sources near an injection site, obviously there cannot be a record of induced seismicity per se before injection begins. New methods are therefore required for evaluating the seismic potential of a given site and its relationship to injection. Any time- and space-dependencies that appear in Steps 1 and 2 must then be rigorously propagated through the entire assessment workflow.

Second, traditional PSRA has focused on building and infrastructure damage, and therefore is primarily concerned with larger events (usually, **M**4.5+). Experience with induced seismicity has extended the range of concern to lower magnitudes (say, **M**2+). The natural earthquake occurrence rate is essentially fixed by tectonic processes and is outside human control. Risk mitigation is

therefore mostly focused on site selection and structural design standards. In induced seismicity, the earthquake occurrence rate is controllable, conceivably, because it is linked to human activities. Therefore, the public has an expectation that the occurrence of *all* induced felt events be kept to a minimum. Frequent felt seismicity will create a community nuisance even if it does not cause damage, and these smaller magnitude events must be a key focus of an expanded risk assessment and management workflow. The inclusion of smaller magnitude events requires important alterations in Steps 3 and 5.

6. Fundamental challenges and recent progress

The previous section has presented a general framework for risk assessment, identifying the key elements that control the seismic hazard and resulting risk. Unfortunately, the inherent complexity of the induced seismicity process introduces technical hurdles that makes the actual implementation of this framework challenging. The next few sections describe several of these underlying challenges, and ongoing efforts aimed at addressing them. These challenges are at the heart of the induced seismicity problem, and novel solutions to them will significantly advance our ability to manage seismic risk during CO_2 injection. The same challenges are relevant to other types of fluid injection as well.

6.1. Fault identification

As described in Section 5, the first step in any seismic risk assessment is source characterization—i.e. identifying individual faults (or faulted zones) that are capable of generating seismicity of concern. Geophysical monitoring techniques have inherent limitations that make detecting faults—particularly smaller faults—difficult. In general, pre-existing faults in proximity to an injection project can be divided into two basic categories: observed and unobserved.

Known faults—such as those mapped at the surface or identified in seismic surveys—can be addressed early in the design phases of a project. The potential for reactivation can be assessed using in situ stress estimates and hydromechanical simulations (Chiaramonte et al., 2014), and hazardous faults can simply be avoided during site selection and project planning. Monitoring and mitigation plans can then be carefully designed around other, lower risk features. Indeed, several carbon storage projects have been sited in close proximity to larger faults—notably Snøhvit (Hansen et al., 2013; Chiaramonte et al., 2014) and Gorgon (Jenkins et al., 2012)—as these faults were deemed low risk. Faults are pervasive in the subsurface, however, and there will always be a population of faults about which little or no information is available prior to injection. A good example of this situation is the Illinois-Basin Decatur Project, where microseismicity has illuminated smaller faults that were not visible in 3D seismic surveys (Will et al., 2014; Couëslan et al., 2014). Assessing and managing the hazard from this unknown fault population is much less straightforward.

The key factor controlling the maximum magnitude event that a fault can produce is its area. At the same time, the likelihood of detecting a fault in the subsurface is also correlated with its size. To illustrate this notion, Fig. 3 plots a commonly-used relationship between rupture diameter, stress drop, and earthquake moment magnitude (Hanks, 1977; Scholz, 2002; Zoback and Gorelick, 2012). This relationship assumes an idealized circular rupture geometry—reasonable for modest earthquakes—so that fault length can be related to a maximum rupture area. This relationship indicates that a fault length of 1 km is potentially capable of generating a maximum earthquake in the **M**3 to **M**4 range. Such events would likely be felt by nearby populations and possibly cause minor damage to seismically fragile infrastructure in the immediate

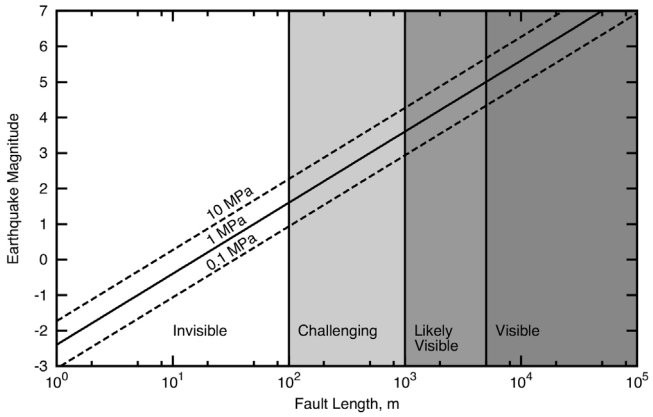

Fig. 3. Scaling relationship between fault rupture length and earthquake magnitude, supported by field observations (Hanks, 1977; Scholz, 2002). Dashed lines indicate a commonly observed range of stress drop, from 0.1 to 10 MPa. Vertical shaded regions indicate "typical" visibility of a given size fault using 3D seismic. Note that actual seismic resolution is highly site, survey, and fault specific, and the depicted thresholds are meant for conceptual illustration only.

vicinity. If the fault intersects the caprock, the rupture could potentially extend several hundred meters vertically through a seal.

A 3D seismic survey, combined with geological and well log data, can be used to detect faults and estimate the maximum magnitude earthquakes that may be expected. There are, however, limitations to fault detectability. For example, while the kilometer-long fault discussed above is large enough to produce seismicity of concern, it is also small enough that it could potentially be missed in seismic interpretation. Fig. 3 shows estimates of fault detectability that might be applicable to a "typical" seismic survey. The specific length ranges shown in Fig. 3 were chosen for illustrative purposes only, as the actual resolution achievable is not only site- and survey-specific, but is also highly dependent on the fault location, geometry and style. The visibility of a fault in a 3D seismic volume is primarily determined by its size and whether it creates detectable vertical offsets on reflecting horizons. Small offsets and steeply dipping faults are particularly difficult to see. Faults that are confined to the basement or to stratigraphic units having widely-spaced reflectors are challenging to detect, as are strike-slip faults, which may have substantial accumulated horizontal displacement but little or no vertical offset.

All carbon storage projects to date have used 3D (and often 4D) seismic as a key component of their site characterization and monitoring plans to provide a significant amount of information about subsurface structure. This is a key distinguishing feature of CO_2 injection compared to many wastewater disposal projects. However, it is critical to assess the resolution achieved with a given survey. A precise understanding of fault detectability will enable regions of lower and higher uncertainty to be distinguished. The injection operation can then be designed to avoid pressure migration into poorly characterized zones.

As mentioned earlier, known faults can be dealt with in the site selection and project design phases, and risk mitigation techniques can be applied. Thus, while the potential hazard from a large fault may be relatively high, the overall risk may be more easily managed. The most common way to obtain information about smaller faults that escape detection during the pre-injection phase is to carefully monitor microseismicity and its relation to pressure evolution in the reservoir as injection proceeds. This, however, creates an unusual situation: we must use the micro-earthquakes themselves to estimate the hazard on an ongoing basis and react rapidly to prevent larger events. We will discuss this issue further below.

While it is often difficult to detect individual faults, fault populations tend to follow well-established statistical distributions in

terms of their size and spatial density (Scholz, 2002). It is sometimes possible to constrain these distributions using available data. In particular, if a data set is available on the density distribution of larger faults—i.e. from geological mapping, 3D seismic, and well observations—it may be possible to extrapolate the observed distribution to estimate the likely density of smaller, unresolved faults. The inferred density can then be used within a probabilistic hazard assessment. Jordan et al. (2011) present an analysis along these lines, using fault density statistics to examine the probability that pressure and/or CO_2 might encounter faults during a previously-planned injection in the San Joaquin Basin. The same approach could be easily extended to assess the resulting seismicity hazard.

6.2. Microseismic event detection, location, and characterization

Microseismic monitoring during injection is the primary tool used to monitor the evolving seismic hazard posed by both known and previously undetected faults. Ideally, the monitoring array can precisely identify, locate, and characterize the micro-earthquakes, but in practice high-quality microseismic monitoring can be a demanding, and often expensive, task. Physical, technological, and budgetary constraints will inevitably limit the resolving power of the array, and introduce significant uncertainties into earthquake source characterization.

The first limitation is often one of cost. The ideal microseismic array would consist of multiple, deep borehole arrays—placing as many geophones as possible in close proximity to the seismic events while simultaneously providing the optimal spatial coverage necessary for accurate location and focal mechanism estimation. Deep borehole deployments are expensive, however, and during the design phases of a project it may not be clear if significant seismicity will even occur. Given budget constraints, project operators must decide whether the money may be better spent monitoring other potential hazards. To date, most projects have opted to deploy a relatively small number of instruments, often using a shallow or deep borehole string (see Table 1). The Illinois-Basin Decatur project is a good example of a monitoring approach in which the monitoring sophistication has adapted to increased understanding of the seismic hazard (White and Foxall, 2014). The initial design of the project began with a baseline microseismic monitoring system, which has subsequently expanded to include two deep borehole arrays (Will et al., 2014) and a separately operated surface network (Kaven et al., 2014, 2015). Recently, there has also been movement towards installing permanent, dual-purpose arrays—i.e. using the same array for both active and passive seismic monitoring. For example, the Aquistore project has deployed a dual-purpose array with 650 geophones spread over a 2.5 km × 2.5 km areal grid (Worth et al., 2014; White et al., 2014a). Looking to the future, significant research investment has focused on innovative technologies that will help lower monitoring cost. These include distributed acoustic sensing fiber-optic technology (Daley et al., 2013), "slimhole" drilling methods, and cheap, easily-deployable surface monitoring systems (Lin et al., 2013; Hutchings et al., 2015b).

Analysis of small-magnitude microseismic events is often plagued by low signal-to-noise ratio and significant uncertainties. Recent research has focused on improved signal processing algorithms in order to extract as much information as possible from recorded waveform data. For example, automated detection algorithms for identifying small magnitude events can extend the completeness of seismicity catalogs that constrain earthquake frequency-magnitude distributions used to estimate the likelihood of larger events. A large body of work on detection and phase arrival picking algorithms exists, e.g. Joswig (1990), Brown et al. (2008), Lomax et al. (2012), Skoumal et al. (2014, 2015) and Yoon et al. (2015). As one example, by applying a Matched Field Processing method (Harris and Kvaerna, 2010; Bucker, 1976; Baggeroer et al., 1993) to data from the Newberry Enhanced Geothermal Field, Templeton et al. (2014) were able to identify 399 microseismic events, compared with 235 detected by a traditional short-term-average/long-term-average method. Similarly, decision-making can be improved when precise event locations (Waldhauser and Ellsworth, 2000; Pujol, 2000; Zhang and Thurber, 2003; Gharti et al., 2010; Soma and Rutledge, 2013) and a good understanding of location uncertainty are available (Myers et al., 2007; Oye et al., 2013; Lomax et al., 2014). Given often non-ideal configurations of monitoring arrays, location uncertainty can be hundreds of meters laterally and vertically.

Additional research efforts are focused on reducing uncertainties in crustal velocity models. For example, Matzel et al. (2014) have recently applied Ambient Noise Correlation—a seismic interferometry technique typically used for imaging large-scale (regional to global) earth structure—to compute accurate 3D velocity and attenuation models beneath dense microseismic arrays. The same group has also applied the Virtual Seismometer Method—a related interferometry technique (Curtis et al., 2009; Hong and Menke, 2006)—to improve focal mechanism estimation based on cross-correlating waveforms recorded for pairs of microseismic events.

6.3. Estimating earthquake recurrence and the influence of injection

As discussed in Section 5, the growing subsurface pressure distribution resulting from injection introduces strong time- and space-dependencies into earthquake occurrence rates, which leads to the hazard evolving with time. New methods are therefore required for evaluating frequency–magnitude distributions in relation to injection. To date, there have been two primary approaches to this: empirically-based methods and simulation-based methods.

Empirically-based methods use a seismicity catalog compiled by microseismic monitoring of the injection to estimate the evolving seismic hazard (Shapiro et al., 2007, 2010; Bachmann et al., 2011; Mena et al., 2013). As the project proceeds, the growing catalog of events is used to continuously re-calibrate the parameters of an earthquake frequency–magnitude model. These empirical approaches typically use simplified models of the underlying physical processes, leading to a manageable number of free parameters to be fitted to observed data. The calibrated model may then be used to forecast the future seismic hazard within some forecast window (Bachmann et al., 2011; Mena et al., 2013). The quality of this forecast will depend on (1) the fidelity of the simplified model to the true system behavior, and (2) the availability of sufficient seismic observations to properly constrain future seismic occurrence. Both aspects of the problem are the subjects of ongoing research.

Most of the recent developments in empirical methods have been applied to reservoir stimulations for enhanced geothermal systems (Shapiro et al., 2007, 2010, 2011; Shapiro, 2015; Bachmann et al., 2011; Mena et al., 2013) where they have shown some promise. A key question, however, is to what extent the underlying physical models translate to geologic carbons storage operations, which operate in higher permeability reservoirs and over much longer time scales. The main limitation in testing these methods for carbon storage has been the lack of field data, though recent data acquisitions (Table 1) are improving this situation. Also, all of these methods make substantial simplifying assumptions that merit further investigation.

Recent work has also explored simulation-based approaches. Numerical simulation has been used to investigate induced seismicity at enhanced geothermal (Baisch et al., 2009; Baisch et al, 2010; McClure and Horne, 2011; Goertz-Allmann and Wiemer,

2013; Gischig and Wiemer, 2013), CO_2 sites (Cappa and Rutqvist, 2011, 2012; Rinaldi et al., 2014; Jha and Juanes, 2014), and wastewater injection systems (Keranen et al., 2014; Dieterich et al., 2015). These modeling approaches have been carried to varying levels of sophistication, but all simulate overpressure that can induce failure on fault elements according to a chosen friction/rupture model. In principle, simulation-based methods can include arbitrarily sophisticated models for the induced seismicity process, and thereby hew more closely to the underlying physics than the simplified empirical models above. In practice, however, obtaining the necessary characterization and calibration data necessary to make these model predictions accurate and useful remains an ongoing challenge.

The maximum magnitude ($\mathbf{M}_{max}$) at which frequency-magnitude distributions are truncated has a significant influence on forecasted hazard (Bachmann et al., 2011), but selection of $\mathbf{M}_{max}$ based on observed data remains an unsolved problem. If faults favorably oriented for failure have been identified intersecting the volume likely to be affected by stress perturbations, then $\mathbf{M}_{max}$ can be estimated from the dimensions of the largest fault. See the related discussion on fault detection in Section 6.1. Failing that, Shapiro et al. (2011) (see also Mena et al. (2013)) have proposed that the magnitude of the largest expected event can be empirically related to the dimensions of the perturbed pressure region. The underlying assumption is that that the maximum magnitude earthquake can occur on an undetected fault having dimensions approximately equal to the dimensions of this perturbed volume. This implicitly assumes that undetected faults of all sizes are pervasive in the vicinity of the injection well, and some are favorably oriented for slip. Since presumably that will not always be the case, it would perhaps be more accurate to say that this approach attempts to place an upper bound on $\mathbf{M}_{max}$ in the absence of more detailed information. McGarr (2014) has also proposed a simple relationship between the upper bound seismic moment and the net cumulative volume of injected fluid. The study notes, however, that the proposed relationship does not place an absolute physical limit on $\mathbf{M}_{max}$. These approaches downplay the possibility that failure of a fault patch within a pressure plume can result in a rupture that continues to propagate outside of it, leading to an event larger than the inferred $\mathbf{M}_{max}$ (Gischig, 2015). Stress transfer from foreshock ruptures and similar long-range perturbations could also promote slip on faults at significant distances from the injection well. An interesting case study here is the 2011 Prague, Oklahoma earthquake sequence attributed to wastewater injection—see Keranen et al. (2013) and Sumy et al. (2014). A **M**5.0 foreshock in close proximity to several wastewater injection wells triggered a complex earthquake cascade in the local fault network. Less than 24 h later, a **M**5.7 mainshock occurred on a fault approximately 2 km away. While the exact controls on this earthquake sequence remain unclear, static stress transfer between the faults may have played an important role.

Another important question from a risk management point of view is to what degree pre-cursor information may be available to identify hazardous situations before they become problematic. Ideally, microseismic observations could indicate a previously unknown fault has been encountered, and this information can be used to revise the seismic hazard estimate and potentially alter injection operations before larger events occur. It is also possible, however, that the largest events will occur very early in the earthquake sequence with little to no warning. In this latter case, "traffic light" systems and injection-rate control techniques may be rendered ineffective (Deichmann and Giardini, 2009; Majer et al., 2012a,b; Walters et al., 2015). As a result, it is important for operators and regulators to include damage mitigation strategies within the project design to ensure practical consequences will be low even if felt earthquakes cannot be prevented.

6.4. Ground motion prediction

A major difference between PSHA for induced and naturally-occurring seismicity is the need to calculate ground motions from small events that do not pose a risk of structural damage, but can be strongly felt at short distances. These events can cause annoyance and alarm, and possibly cosmetic damage. Depending on the distance to nearby communities, magnitudes as low as **M**1.5–**M**2 may need to be included in the hazard analysis.

Traditional PSHA employs empirical ground motion prediction equations (GMPEs) derived by regressions on worldwide strong motion data (Abrahamson and Shedlock, 1997; Abrahamson et al., 2008; Bozorgnia et al., 2014). The majority of existing GMPEs do not extend to magnitudes below **M**4.5, and even then are poorly constrained for smaller events and short distances (Bommer et al., 2006). The most recent GMPEs developed by the Pacific Earthquake Engineering Research Center Next Generation Attenuation (NGA) Working Group, NGA-West2, has been extended to **M**3.0 (Bozorgnia et al., 2014). However, the empirical fits are constrained by only minimal observed data from events smaller than **M**6 at distances less than 5 km. Douglas et al. (2013) recently developed GMPEs specifically for magnitudes less than **M**3.5 based on data from six geothermal areas worldwide, but the aleatory uncertainties on these generic relationships are quite large, owing primarily to site-to-site variability.

Microearthquake seismograms from small earthquakes can be used as empirical Green's functions (EGFs) for site-specific calculation of ground motion from larger events (e.g. Hutchings et al., 2007; Hutchings and Wu, 1990). The EGFs contain complete information about the point-source response (wave propagation) of the Earth along specific source-site paths. Larger events are modeled as a composite sequence of point-source sub-events on the fault plane that propagates at the earthquake rupture velocity. The ground motions at specific sites are calculated by convolving each point-source with the appropriate EGFs and summing the in-phase contributions from all of the sub-events.

Prior to injection, when in most cases recorded microearthquakes that could used as EGFs will not be available, it may be necessary to develop synthetic Green's functions. These are calculated by analytically or numerically modeling wave propagation from an array of synthetic point sources through the local seismic velocity and attenuation structure (Graves and Pitarka, 2010, 2015; Hutchings et al., 2015a). The accuracy of the synthetic functions will clearly depend on the quality of site characterization data available. Another method of deriving Green's functions and crustal velocity structure without microearthquake recordings is Ambient Noise Tomography, which has recently been applied in local-scale studies in (Matzel et al., 2014).

Ground acceleration and velocity amplitudes at a specific receiver site are strongly influenced by amplification effects that depend on the near-surface geology. Conventionally, amplification factors are applied to bedrock ground motions based on broad site classifications, often parameterized in terms of the average S-wave velocity above a depth of 30 m (VS30). Inversion methods have also been developed to obtain site response spectral amplifications from ambient noise recordings (Herak et al., 2008) and near-surface velocity profiles (Scherbaum et al., 2003). One approach is to use near-surface-velocity profiles to calculate analytic Green's functions, which are then convolved with site response functions to obtain site-specific Green's functions (Scognamiglio and Hutchings, 2009).

6.5. Structural and community vulnerability

The effects of ground-motion produced by medium to large earthquakes (**M**4.5+) on structures are usually modeled with a

fragility function that expresses the probability of structural damage as a function of ground-motion acceleration or velocity, or seismic intensity. These are combined with hazard curves to calculate damage risk; i.e. the probability of exceeding given damage levels at a site over a specified time period. Standard fragility functions can be applied to assess structural damage from either natural or induced earthquakes (e.g. U.S. Federal Emergency Management Agency, 2013).

Because smaller magnitude events are a key consideration for induced seismicity, an equivalent methodology must be developed to address the risk of nuisance and the attendant impact on public perception. The effects of felt but non-damaging ground motions have been extensively studied in the context of vibrations generated by mining and construction, which has led to the development of national (e.g. American National Standards Institute) and international (International Standards Organization) standards in the form of deterministic acceptability criteria (Dowding, 1996). These acceptability criteria form the basis for a U.S. Department of Energy protocol for assessing and mitigating nuisance risk created by enhanced geothermal systems (Majer et al., 2012a,b). These DOE guidelines could also generally be applied to CO_2-induced ground motions. Further work is needed to determine the most appropriate ground motion metric (acceleration, velocity, etc.) to relate to human response.

With regard to nuisance potential, an injection project's community outreach efforts (or lack there of) may have an important impact on how the local community reacts to seismicity. A project that is widely-perceived to provide tangible benefit to the community—e.g. by providing employment opportunities, economic stimulus, or environmental benefits—may be given more leeway than a project that is viewed with widespread skepticism. Similarly, a community's general familiarity with carbon storage technology is an important factor in the public perception of its riskiness (Singleton et al., 2009). A model case study in this context is the Geyser's Geothermal Project, which has a well-developed public education and outreach program aimed at local residents (Dobson, 2014; National Research Council, 2012). Clearly, however, building public trust and familiarity requires a focused and long-term commitment.

7. Conclusion

The goal of this paper has been to identify and describe specific technical difficulties that make seismic risk assessments for CO_2 storage operations inherently challenging. In our view, these issues lie at the heart of the induced seismicity problem, and focused research is required to address them. While promising progress has been made to date, a number of hurdles remain. These may be briefly summarized as follows:

1. Faults are pervasive in the subsurface, with a large range of scales, and our ability to identify and characterize them through geophysical techniques is inherently limited. Moderate-sized faults pose the greatest challenge, as they are both large enough to produce seismicity of concern but small enough to be often hard to detect via traditional means. Improved techniques for identifying and characterizing potential seismic sources are therefore needed. These techniques must be cost effective, practical to deploy, and allow for a quick turn-around time between data collection and interpretation.
2. The relationship between injection rate and seismic activity is complex, site-specific, and also constantly evolving in time and space. Project operators have limited time to understand and react to these evolving hazards. Better data analysis and modeling techniques, soundly based on the physics of induced seismicity, are therefore required to characterize earthquake occurrence relationships and their connection to injection operations.
3. Because felt events resulting from injection activities have the potential to alarm or annoy nearby communities, the lower bound magnitude of concern for induced seismicity (about **M**1.5–**M**2) is lower than that typically focused on for natural seismic risk assessment (usually ~**M**4.5). Conventional seismic risk assessment methods must therefore be updated to address smaller events, shorter distances, and the risk of nuisance in addition to property damage. Further, the intrinsic spatial- and time-dependencies introduced by the hydromechanical processes responsible for induced seismicity will have an important impact on the risk assessment workflow.
4. While not a focus of this paper, it should be recognized that risk management techniques for controlling seismicity and associated impacts have inherent limitations. There can also often be a significant delay before control measures take effect. As a simple example, drawing down the pressure in a reservoir can be effective at controlling seismicity, but will take time for pressure changes to propagate significant distances from injection or production wells. In this context, risk assessment techniques should ideally be predictive, allowing operators to assess how different operational decisions will impact forecasted seismic risk. This ability to look ahead is essential for proactive, rather than purely reactive, risk management.
5. Even though the overall number of CO_2 injection projects is growing, relatively few investigations have been undertaken on the seismic behavior of these fields. Moving forward, more observational data and field experience is clearly necessary. Further, it is important that this data be made broadly-accessible to independent research groups to solicit the best analysis and insight available.

Experience with induced seismicity at carbon storage sites is limited, and best practices will likely evolve as field experience grows. While seismicity is a serious concern and should be carefully addressed by all future projects, evidence to date at several successful projects suggests that good site selection and careful project design can lower seismic risk to acceptably low levels. Deploying CO_2 storage at sufficient scale to significantly impact global greenhouse gas emissions will require a dramatic scale-up in the number of storage projects, however, and well-focused research can help ensure we deploy this new infrastructure in a safe and responsible manner.

Acknowledgements

This work was completed as part of the National Risk Assessment Partnership (NRAP) project. Support for this project came from the U.S. Department of Energy, Office of Fossil Energy, Cross-Cutting Research Program. This work was performed by Lawrence Livermore National Laboratory for the Department of Energy under contract number DE-AC52-07NA27344 and by Lawrence Berkeley National Laboratory under contract number DE-AC02-05CH11231.

References

Abrahamson, N., Shedlock, K., 1997. Overview. Seismol. Res. Lett. 68, 9–23.
Abrahamson, N., et al., 2008. Comparisons of the NGA ground-motion relations. Earthquake Spectra 24 (1), 45–66.
Ake, J., Mahrer, K., O'Connell, D., Block, L., 2005. Deep-injection and closely monitored induced seismicity at Paradox Valley, Colorado. Bull. Seismol. Soc. Am. 95 (2), 664–683.
Bachmann, C., et al., 2011. Statistical analysis of the induced Basel 2006 earthquake sequence: introducing a probability-based monitoring approach for enhanced geothermal systems. Geophys. J. Int. 186 (2), 793–807.
Baggeroer, A.B., Kuperman, W.A., Mikhalevsky, P.N., 1993. Matched field processing in ocean acoustics. In: Moura, J.M.F., Lourtie, I.M.G. (Eds.),

Proceedings of the NATO Advanced Study Institute on Signal Processing for Ocean Exploration. Kluwer, Dordrecht, Netherlands.
Baisch, S., et al., 2009. Deep Heat Mining Basel-Seismic Risk Analysis. Technical Report. Serianex.
Baisch, S., et al., 2010. A numerical model for fluid injection induced seismicity at Soultz-sous-Forets. Int. J. Rock Mech. Mining Sci. 47 (3), 405–413.
Block, L., et al., 2012. Review of geologic investigations and injection well site selection, Paradox Valley Unit, Colorado. U.S. Bureau of Reclamation, Technical Memorandum 86-68330-2012-27, 71 pp.
Bommer, J.J., et al., 2006. Control of hazard due to seismicity induced by a hot fractured rock geothermal project. Eng. Geol. 83 (4), 287–306.
Bozorgnia, Y., et al., 2014. NGA-West2 research project. Earthquake Spectra 30 (3), 973–987.
Brown, J.R., Beroza, G.C., Shelly, D.R., 2008. An autocorrelation method to detect low frequency earthquakes within tremor. Geophys. Res. Lett. 35 (16), L16305, http://dx.doi.org/10.1029/2008GL034560.
Bucker, H.P., 1976. Use of calculated sound field and matched-field detection to locate sound sources in shallow water. J. Acoust. Soc. Am. 59 (2), 368–373.
Cappa, F., Rutqvist, J., 2011. Modeling of coupled deformation and permeability evolution during fault reactivation induced by deep underground injection of CO_2. Int. J. Greenh. Gas Control 5, 336–346, http://dx.doi.org/10.1016/j.ijggc.2010.08.005.
Cappa, F., Rutqvist, J., 2012. Seismic rupture and ground accelerations induced by CO_2 injection in the shallow crust. Geophys. J. Int. 190 (3), 1784–1789.
Chiaramonte, L., White, J.A., Trainor-Guitton, W., 2014. Probabilistic geomechanical analysis of compartmentalization at the Snøhvit CO_2 sequestration project. J. Geophys. Res. Solid Earth 120, http://dx.doi.org/10.1002/2014JB011376.
Couëslan, M.L., et al., 2014. Integrated reservoir monitoring at the Illinois Basin-Decatur Project. Energy Proc. 63, 2836–2847.
Curtis, A., et al., 2009. Virtual seismometers in the subsurface of the Earth from seismic interferometry. Nat. Geosci. 2, 700–704.
Daley, T.M., et al., 2013. Field testing of fiber-optic distributed acoustic sensing (DAS) for subsurface monitoring. Leading Edge, 936–942.
Davis, S.D., Pennington, W.D., 1989. Induced seismic deformation in the Cogdell oil field of west Texas. Bull. Seismol. Soc. Am. 79 (5), 1477–1495.
Deichmann, N., Giardini, D., 2009. Earthquakes induced by the stimulation of an enhanced geothermal system below Basel (Switzerland). Seismol. Res. Lett. 80 (5), 784–798.
Dieterich, J.H., 1979. Modeling of rock friction. 1. Experimental results and constitutive equations. J. Geophys. Res. 84 (B5), 2161–2168.
Dieterich, J.H., Richards-Dinger, K.B., Kroll, K.A., 2015. Modeling injection-induced seismicity with the physics-based earthquake simulator RSQSim. Seismol. Res. Lett. 86 (4), 1058–1059, http://dx.doi.org/10.1785/0220150057.
Dobson, P.F., 2014. Calpine geothermal visitor center upgrade project: an interactive approach to geothermal outreach and education at The Geysers. Geothermal Res. Council Trans. 36, 399–405.
Douglas, J., et al., 2013. Predicting ground motion from induced earthquakes in geothermal areas. Bull. Seismol. Soc. Am. 103, 1875–1897.
Dowding, C., 1996. Construction Vibrations. Prentice Hall.
Gan, W., Frohlich, C., 2013. Gas injection may have triggered earthquakes in the Cogdell Oil Field, Texas. Proc. Natl. Acad. Sci. U.S.A. 110 (47), 18786–18791.
Gharti, H.N., et al., 2010. Automated microearthquake location using envelope stacking and robust global optimization. Geophysics 75 (4), MA27–MA46, http://dx.doi.org/10.1190/1.3432784.
Gischig, V., Wiemer, S., 2013. A stochastic model for induced seismicity based on non-linear pressure diffusion and irreversible permeability enhancement. Geophys. J. Int. (194), 1229–1249.
Gischig, V., 2015. Rupture propagation behavior and the largest possible earthquake induced by fluid injection into deep reservoirs. Geophys. Res. Lett. 42, 7420–7428.
Goebel, TH.W., et al., 2015. An objective method for the assessment of fluid injection-induced seismicity and application to tectonically active regions in central California. J. Geophys. Res. Solid Earth 120, 7013–7032.
Goebel, TH.W., 2015. A comparison of seismicity rates and fluid-injection operations in Oklahoma and California: implications for crustal stresses. Leading Edge, 640–648.
Goebel, T.H.W., et al., 2016. Wastewater disposal and earthquake swarm activity at the southern end of the Central Valley, California. Geophys. Res. Lett. 43, http://dx.doi.org/10.1002/2015GL066948.
Goertz-Allmann, B.P., Wiemer, S., 2013. Geomechanical modeling of induced seismicity source parameters and implications for seismic hazard assessment. Geophysics 78, KS25–KS39.
Goertz-Allmann, B.P., et al., 2014. Combining microseismic and geomechanical observations to interpret storage integrity at the In Salah CCS site. Geophys. J. Int., http://dx.doi.org/10.1093/gji/ggu010.
Graves, R., Pitarka, A., 2010. Broadband ground-motion simulation using a hybrid approach. Bull. Seismol. Soc. Am. 100, 2095–2123.
Graves, R., Pitarka, A., 2015. Refinements to the Graves and Pitarka (2010) broadband ground-motion simulation method. Seismol. Res. Lett. 86, 75–80.
Han, W.S., et al., 2010. Evaluation of trapping mechanisms in geologic CO_2 sequestration: case study of SACROC northern platform, a 35-year CO_2 injection site. Am. J. Sci. 310 (4), 282–324, http://dx.doi.org/10.2475/04.2010.03.
Hanks, T.C., 1977. Earthquake stress drops, ambient tectonic stresses and stresses that drive plate motions. Pure Appl. Geophys. 115 (1-2), 441–458.
Hansen, O., et al., 2013. Snøhvit: the history of injecting and storing 1 Mt CO_2 in the Fluvial Tubåen Fm. Energy Proc. 37, 3565–3573.
Harris, D.B., Kvaerna, T., 2010. Superresolution with seismic arrays using empirical matched field processing. Geophys. J. Int. 182, 1455–1477.
Herak, M., 2008. ModelHSVR: a Matlab tool to model horizontal-to-vertical spectral ratio of ambient noise. Comput. Geosci. 34, 1514–1526.
Hong, T.-K., Menke, W., 2006. Tomographic investigation of the wear along the San Jacinto fault, southern California. PEPI 155, 236–248.
Hutchings, L., et al., 2007. A physically based strong ground-motion prediction methodology; application to PSHA and the 1999 M = 6.0 Athens earthquake. Geophys. J. Int. 168, 569–680.
Hutchings, L., Wu, F., 1990. Empirical Green's functions from small earthquakes: a waveform study of locally recorded aftershocks of the 1971 San Fernando Earthquake. J. Geophys. Res. 95, 1187–1214.
Hutchings, L., et al., 2015a. Examination of a site-specific, physics-based seismic hazard analysis, applied to surrounding communities of The Geysers geothermal development area. Geothermal Resour. Council Trans. 39, 615–626.
Hutchings, L., et al.,2015b. Micro-earthquake analysis for reservoir properties at the Prati-32 injection test, The Geysers, California. In: Proc. 40th Workshop on Geothermal Reservoir Engineering. Stanford University, California, January 26–28, abstract SGP-TR-204.
International Energy Agency Greenhouse Gas R&D Programme (IEAGHG), 2013. Induced Seismicity and Its Implications for CO_2 Storage Risk. Report No. 2013/09.
International Energy Agency, 2010. Energy Technology Perspectives 2010: Scenarios and Strategies to 2050, 20 pp.
Imbus, S.W., et al., 2013. CO_2 storage contingencies initiative: detection, intervention and remediation of unexpected CO_2 migration. Energy Proc. 37, 7802–7814.
Jenkins, C.R., et al., 2012. Safe storage and effective monitoring of CO_2 storage in depleted gas fields. Proc. Natl. Acad. Sci. U.S.A. 109 (2), E35–E41.
Jha, B., Juanes, R., 2014. Coupled multiphase flow and poromechanics: a computational model of pore pressure effects on fault slip and earthquake triggering. Water Resour. Res. 50 (5), 3776–3808.
Jordan, P., Oldenburg, C., Nicot, J.-P., 2011. Estimating the probability of CO_2 plumes encountering faults. Greenh. Gases: Sci. Technol. 1, 160–174.
Joswig, M., 1990. Pattern recognition for earthquake detection. Bull. Seismol. Soc. Am. 80 (1), 170–186.
Juanes, R., Hager, B.H., Herzog, H.J., 2012. No geologic evidence that seismicity causes fault leakage that would render large-scale carbon capture and storage unsuccessful. Proc. Natl. Acad. Sci. U.S.A. 109 (52), E3623.
Kaplan, S., Garrick, B.J., 1981. On the quantitative definition of risk. Risk Anal. 1 (1), 11–27.
Kaven, J.O., et al., 2014. Seismic monitoring at the Decatur, IL, CO_2 sequestration demonstration site. Energy Proc. 63, 4264–4272.
Kaven, J.O., et al., 2015. Surface monitoring of microseismicity at the Decatur, Illinois, CO_2 sequestration demonstration site. Seismol. Res. Lett. 86 (4), 1096–1101.
Keranen, K., et al., 2013. Potentially induced earthquakes in Oklahoma, USA: links between wastewater injection and the 2011 MW 5.7 earthquake sequence. Geology, http://dx.doi.org/10.1130/G34045.
Keranen, K.H., et al., 2014. Sharp increase in central Oklahoma seismicity since 2008 induced by massive wastewater injection. Science 345, 448–451.
Lin, F-C., et al., 2013. High-resolution 3D shallow crustal structure in Long Beach, California: application of ambient noise tomography on a dense seismic array. Geophysics 78, Q45–Q56.
Lomax, A., Satriano, C., Vassallo, M., 2012. Automatic picker developments and optimization: FilterPicker – a robust, broadband picker for real-time seismic monitoring and earthquake early warning. Seismol. Res. Lett. 83, 531–540.
Lomax, A., Michelini, A., Curtis, A., 2014. Earthquake location, direct, global-search methods. In: Meyers, R.A. (Ed.), Encyclopedia of Complexity and System Science. , 2nd ed. Springer, New York, pp. 2449–2473.
Majer, E., et al., 2012a. Protocol for Addressing Induced Seismicity Associated with Enhanced Geothermal Systems. US Department of Energy, DOE EE-0662.
Majer, E., et al., 2012b. Best Practices for Addressing Induced Seismicity Associated with Enhanced Geothermal Systems (EGS). Draft Report prepared for the DOE Geothermal Technologies Program. Lawrence Berkeley National Laboratory.
Matzel, E., et al., 2014. Microseismic techniques for avoiding induced seismicity during fluid injection. Energy Proc. 63, 4297–4304.
McClure, M.W., Horne, R.N., 2011. Investigation of injection-induced seismicity using a coupled fluid flow and rate/state friction model. Geophysics 76 (6), WC181–WC198.
McGarr, A., 2014. Maximum magnitude earthquakes induced by fluid injection. J. Geophys. Res. 119 (2), 1008–1019, http://dx.doi.org/10.1002/2013JB010597.
Mena, B., Wiemer, S., Bachmann, C., 2013. Building robust models to forecast the induced seismicity related to geothermal reservoir enhancement. Bull. Seismol. Soc. Am. 103 (1), 383–393.
Myers, S.C., Johannesson, G., Hanley, W., 2007. A Bayesian hierarchical method for multiple-event seismic location. Geophys. J. Int. 171, 1049–1063.
National Research Council, 2012. Induced Seismicity Potential in Energy Technologies. National Academies Press, 238 pp.
Oye, V., et al., 2013. Microseismic monitoring and interpretation of injection data from the In Salah CO_2 storage site (Krechba), Algeria. Energy Proc. 37, 4191–4198.
Pacala, S., Socolow, R., 2004. Stabilization wedges: solving the climate problem for the next 50 years with current technologies. Science 305 (5686), 968–972.

Pawar, R.J., et al., 2015. Recent advances in risk assessment and risk management of geologic CO_2 storage. Int. J. Greenh. Gas Control 40, 292–311, http://dx.doi.org/10.1016/j.ijggc.2015.06.014.
Pujol, J., 2000. Joint Event Location–The JHD Technique and Applications to Data from Local Seismic Networks. Advances in Seismic Event Location. Springer, Netherlands, pp. 163–204.
Rinaldi, A., Rutqvist, J., Cappa, F., 2014. Geomechanical effects on CO_2 leakage through fault zones during large-scale underground injection. Int. J. Greenh. Gas Control 20, 117–131.
Rubinstein, J.L., Ellsworth, W.L., McGarr, A., Benz, H.M., 2014. The 2001-present induced earthquake sequence in the Raton Basin of northern New Mexico and southern Colorado. Bull. Seismol. Soc. Am. 104 (5), 2162–2181.
Ruina, A., 1983. Slip instability and state variable friction laws. J. Geophys. Res. 88 (10), 359–410.
Rutledge, J.T., 2010. Geologic demonstration at the Aneth Oil Field, Paradox Basin, Utah. Southwest Regional Partnership on Carbon Sequestration Phase II Topical Report., http://dx.doi.org/10.2172/1029292, 229 pp.
Scherbaum, F., Hinzen, K-G., Ohrnberger, M., 2003. Determination of shallow shear wave velocity profiles in the Cologne, Germany area using ambient vibrations. Geophys. J. Int. 152, 597–612.
Scholz, C.H., 2002. The Mechanics of Earthquakes and Faulting. Cambridge University Press.
Scognamiglio, L., Hutchings, L., 2009. A test of a physically-based strong ground motion prediction methodology with the 27 September 1997, Mw = 6.0 Colfiorito (Umbria-Marcha sequence), Italy earthquake. Tectonophysics 476, 145–158.
Segall, P., 1989. Earthquakes triggered by fluid extraction? Geology 17 (10), 942–946.
Shapiro, S.A., 2015. Fluid-Induced Seismicity. Cambridge University Press.
Shapiro, S.A., et al., 2010. Seismogenic index and magnitude probability of earthquakes induced during reservoir fluid stimulations. Leading Edge 29 (3), 304–309.
Shapiro, S.A., et al., 2011. Magnitudes of induced earthquakes and geometric scales of fluid-stimulated rock volumes. Geophysics 78, WC55–WC63.
Shapiro, S.A., Dinske, C., Kummerow, J., 2007. Probability of a given-magnitude earthquake induced by a fluid injection. Geophys. Res. Lett. 34 (22), http://dx.doi.org/10.1029/2007GL031615.
Singleton, G., Herzog, H., Ansolabehere, S., 2009. Public risk perspectives on geologic storage of carbon dioxide. Int. J. Greenh. Gas Control 3, 100–107.
Skoumal, R.J., Brudinski, M.R., Currie, B.S., Levy, J., 2014. Optimizing multi-station earthquake template matching through re-examination of the Youngstown, Ohio, sequence. Earth Planet. Sci. Lett. 405, 274–280.
Skoumal, R.J., Brudinski, M.R., Currie, B.S., Levy, J., 2015. Corrigendum to 'Optimizing multi-station earthquake template matching through re-examination of the Youngstown, Ohio, sequence'. Earth Planet. Sci. Lett. 410, 210.
Soma, N., Rutledge, J.T., 2013. Relocation of micro seismicity using reflected waves from single-well, three-component array observations: application to CO_2 injection at the Aneth oil field. Int. J. Greenh. Gas Control 19, 74–91.
Sumy, D.F., et al., 2014. Observations of static Coulomb stress triggering of the November 2011 M5.7 Oklahoma earthquake sequence. J. Geophys. Res. Solid Earth 119 (3), 1904–1923.
Templeton, D.C., Johannesson, G., Myers, S.C.,2014. An investigation of the microseismicity at the Newberry EGS site. In: Proc. 39th Workshop on Geothermal Reservoir Engineering. Stanford University, California, January 24–26, abstract SGP-TR-202.
U.S. Environmental Protection Agency, 2012. Geologic Sequestration of Carbon Dioxide: Underground Injection Control (UIC) Program Class VI Well Project Plan Development Guidance, EPA 816-R-11-017. http://water.epa.gov/type/groundwater/uic/class6/gsguidedoc.cfm (accessed 15.10.15).
U.S. Federal Emergency Management Agency, 2013. Methodology for Estimating Potential Losses from Disasters. http://www.fema.giv/hazus/#3 (accessed 15.10.15).
Verdon, J.P., et al., 2010. Passive seismic monitoring of carbon dioxide storage at Weyburn. The Leading Edge.
Verdon, J.P., et al., 2011. Linking microseismic event observations with geomechanical models to minimize the risks of storing CO_2 in geological formations. Earth Planet. Sci. Lett. 205, 143–152.
Verdon, J.P., et al., 2015. Simulation of seismic events induced by CO_2 injection at In Salah, Algeria. Earth Planet. Sci. Lett. 426, 118–129.
Vilarrasa, V., Carrera, J., 2015a. Reply to Zoback and Gorelick: geologic carbon storage remains a safe strategy to significantly reduce CO_2 emissions. Proc. Natl. Acad. Sci. U.S.A. 112 (33), E4511.
Vilarrasa, V., Carrera, J., 2015b. Geologic carbon storage is unlikely to trigger large earthquakes and reactivate faults through which CO_2 could leak. Proc. Natl. Acad. Sci. U.S.A. 112 (9), 5938–5943.
Waldhauser, F., Ellsworth, W.L., 2000. A double-difference earthquake location algorithm: method and application to the northern Hayward fault, California. Bull. Seismol. Soc. Am. 90 (6), 1353–1368.
Walters, R.J., et al., 2015. Characterizing and responding to seismic risk associated with earthquakes potentially triggered by fluid disposal and hydraulic fracturing. Seismol. Res. Lett., http://dx.doi.org/10.1785/0220150048.
Weingarten, M., et al., 2015. High-rate injection is associated with the increase in U.S. mid-continent seismicity. Science 348, 1336–1340.
White, D.J., et al., 2011. Geophysical monitoring of the Weyburn CO_2 flood: results during 10 years of injection. Energy Proc. 4, 3628–3635, http://dx.doi.org/10.106/j.egypro.2011.02.293.
White, D.J., et al., 2014a. Initial results from seismic monitoring at the Aquistore CO_2 storage site, Saskatchewan, Canada. Energy Proc. 63, 4418–4423.
White, J.A., et al., 2014b. Geomechanical behavior of the reservoir and caprock system at the In Salah CO_2 storage project. Proc. Natl. Acad. Sci. U.S.A. 111 (24), 8747–8752.
White, J.A., Foxall, W., 2014. A phased approach to induced seismicity risk management. Energy Proc. 63, 4841–4849.
Whittaker, S., et al., 2011. A decade of CO_2 injection into depleting oil fields: monitoring and research activities of the IEA GHG Weyburn–Midale CO_2 Monitoring and Storage Project. Energy Proc. 4, 6069–6076.
Will, R., et al., 2014. Microseismic monitoring, event occurrence, and the relationship to subsurface geology. Energy Proc. 63, 4424–4436.
Worth, K., et al., 2014. Aquistore project measurement, monitoring, and verification: from concept to CO_2 injection. Energy Proc. 63, 3202–3208.
Yoon, C.E., et al., 2015. Earthquake detection through computationally efficient similarity search. Sci. Adv. 1 (11), e1501057, http://dx.doi.org/10.1126/sciadv.1501057.
Zahasky, C., Benson, S.M., 2014. Evaluation of the effectiveness of injection termination and hydraulic controls for leakage containment. Energy Proc. 63, 4666–4676.
Zhang, H., Thurber, C.H., 2003. Double-difference tomography: the method and its application to the Hayward fault, California. Bull. Seismol. Soc. Am. 93, 1875–1889.
Zhou, R., Huang, L., Rutledge, J.T., 2010. Microseismic event location for monitoring CO_2 injection using double difference tomography. Leading Edge.
Zoback, M.D., Townend, J., 2001. Implications of hydrostatic pore pressures and high crustal strength for deformation of intraplate lithosphere. Tectonophysics 336, 19–30.
Zoback, M.D., Gorelick, S.M., 2012. Earthquake triggering and large-scale geologic storage of carbon dioxide. Proc. Natl. Acad. Sci. U.S.A. 109 (26), 10164–10168.
Zoback, M.D., Gorelick, S.M., 2015. To prevent earthquake triggering, pressure changes due to CO_2 injection need to be limited. Proc. Natl. Acad. Sci. U.S.A. 112 (33), E4510.